Three-Dimensional Visualization and Animation for Power Systems Analysis

Federico Milano [a,*]

[a] *Department of Electrical Engineering of the University of Castilla-La Mancha, 13071, Ciudad Real, Spain*

Abstract

This paper describes a novel approach for three-dimensional visualization and animation of power systems analyses. The paper demonstrates that three-dimensional visualization of power systems can be used for teaching and can help in easily understanding complex concepts. The solutions of power flow analysis, continuation power flow, optimal power flow and time domain simulations are used for illustrating the proposed technique. The paper presents a variety of examples, particularly oriented to education and practitioner training. Conclusions are duly drawn.

Key words:
Three-dimensional visualization, animation, power system analysis, time domain simulation, continuation power flow, optimal power flow.

1 Introduction

1.1 Motivation

The visualization of the results of power system simulations has been limited so far to bi-dimensional plots of state and algebraic variables versus time or some other relevant parameters (e.g., the loading factor in continuation power flow analysis). This way of visualizing system transients and parametric analyses requires a previous knowledge of the network topology in order to fully understand the system behavior. In other words, conventional two-dimensional

* Corresponding author
Email address: `Federico.Milano@uclm.es` (Federico Milano).

plots requires a relatively high level of abstraction in order to get the full picture of the system. This level can be reached with practice and experience by practitioners that run simulations on a daily basis, but can be hardly obtained by students of undergraduate courses. Even for graduate students, the process of familiarising with system transients typically requires a relevant time of their Ph.D. courses.

In several other fields of engineering applications (e.g., civil engineering, mechanics, chemistry, etc.), three-dimensional (3D) plots and animations have been introduced years ago. We believe that time is ready to upgrade power system visualization and propose full 3D, full coloured, animated plots. In this paper, we present and describe in detail how 3D plots and animations are able to show state and algebraic variables as well as the topology of the power system.

1.2 Literature Review

The importance of an intuitive and fully informative visualization of power system results has been recognized and formalized in early nineties. In [1], the authors specifies three guidelines for setting up a good graphical representation of a physical phenomena: (i) natural encoding of information; (ii) task specific graphics; and (iii) no gratuitous graphics. In [2, 3], two-dimensional contour plots are proposed for the visualization of voltage bus levels with inclusion of the topological information of the network. The contour plot complies with the three guidelines mentioned above. In this paper the idea of using contour plots proposed in [2] is extended to three dimensions. Furthermore, 3D animation is used to show electromechanical transients and continuation power flow analysis.

In [4–9], the contour plot technique is further developed for visualizing a variety of data, such as power flows in transmission lines, locational marginal prices, available transfer capability, contingency analysis, etc. All these references focus on static data visualization and are basically two-dimensional plots. A simple animation is provided for visualising the effect of load power variations. The flows are represented by moving arrows in the topological scheme, and transmission line and transformer saturation is indicated by means of pie charts. Three-dimensional representation is limited to coloured "thermometers" on top of the network scheme. The tool described in [4–9] is proprietary software and cannot be customized or freely distributed.

3D visualization has not been exploited so far for power system analysis, although in [10], the advantages of the 3D visualization are discussed and recognized. In [11], rotor speeds of a multi-machine system are displayed in a kind of 3D plot, however the topological information is missing. Reference [12] proposes a variety of 3D visualizations and animations of traveling waves in transmission lines. In [12], the third dimension is used to display the topology and the animation to represent time evolution. This paper extends the approach given in [12] to electromechanical transients as well as to other stability and economical analyses of power systems. The applications of the proposed visualization approach are especially suited for, but not limited to, teaching power systems. The main focus of education is not proposing new technical ideas, but rather to propose novel approaches for easing the learning process of well-assessed concepts.

1.3 Contributions

In summary, the contributions of this paper are:

(1) A novel approach for 3D visualization and animation of a variety of power system analyses, including power flow, continuation power flow, optimal power flow and time domain simulations.
(2) A technique that can help power engineering students, practitioners and also non-technical people in understanding the behavior and the operation of electrical energy systems.

1.4 Paper Organization

This paper is organized as follows. Section 2 describes the proposed 3D visualization and the author's teaching experience using 3D maps. Section 3 presents several illustrative examples of 3D visualization and animation of power system simulations through a variety of test case networks. The differences and the advantages of the proposed visualizations with respect conventional plots are discussed in detail. For the sake of clarity, Section 3 also briefly introduces the power flow, the optimal power flow, the continuation power flow, and the time domain integration. Section 4 draws relevant conclusions. Finally, Appendix A briefly introduce the software tool used for the simulations.

2 Proposed Visualization Technique

The basic functioning of the proposed tool is depicted in Fig. 1. The 3D visualization needs two sources, one for topological data and another one for model/numerical data. These two sources are independent and are not neces-

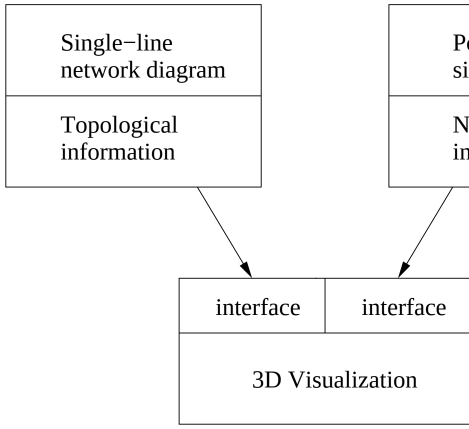

Fig. 1. Basic functioning of the 3D visualization tool.

sarily part of the same software package. Some further implementation details are provided in Appendix A.

3D plot have been obtained by computing the convex hull that envelopes the values obtained from the simulations into a thee-dimensional surfaces with high resolution. For example, let us consider the bus voltage levels of the power network. The number of available voltage values is equal to the number of buses, which is typically not sufficiently high to adequately fill the surface up. To overcome this issue, we created a grid with a high number of points and then assign a value (or a "height") to each point of a 2D grid through polynomial interpolation. The third dimension, i.e. the high of each point of the grid, is then determined by solving the convex hull problem and Delaunay triangulation. The resulting surface is finally coloured using a contour map. The last step consists in superposing the one-line diagram of the network over the surface obtained by the triangulation. Some further detail on the convex hull problem and relevant bibliography are given in Appendix B.

The result of the procedure described above is shown in Fig. 2. In this case, Matlab has been used to compute the Delaunay triangulation and plot results. The "thermometer" on the right side of the plot indicates the p.u. levels of voltage magnitudes.

A feature of 3D objects is that one can choose the point of view of the surface. This can help in getting a more complete understanding of the results, as further discussed in the next session. A byproduct of the proposed technique is that the 3D surface can be also displayed as a 2D plot by just placing the point of view at the zenith of the surface, thus obtaining a contour plot similar to those presented in [2] (see Fig. 3). Thus, the proposed technique includes as a particular case 2D temperature maps as proposed in the literature [4–9].

For producing 3D animations, several plots are stored for each simulation (see Fig. 4). The process is similar to the one described for static 3D contour

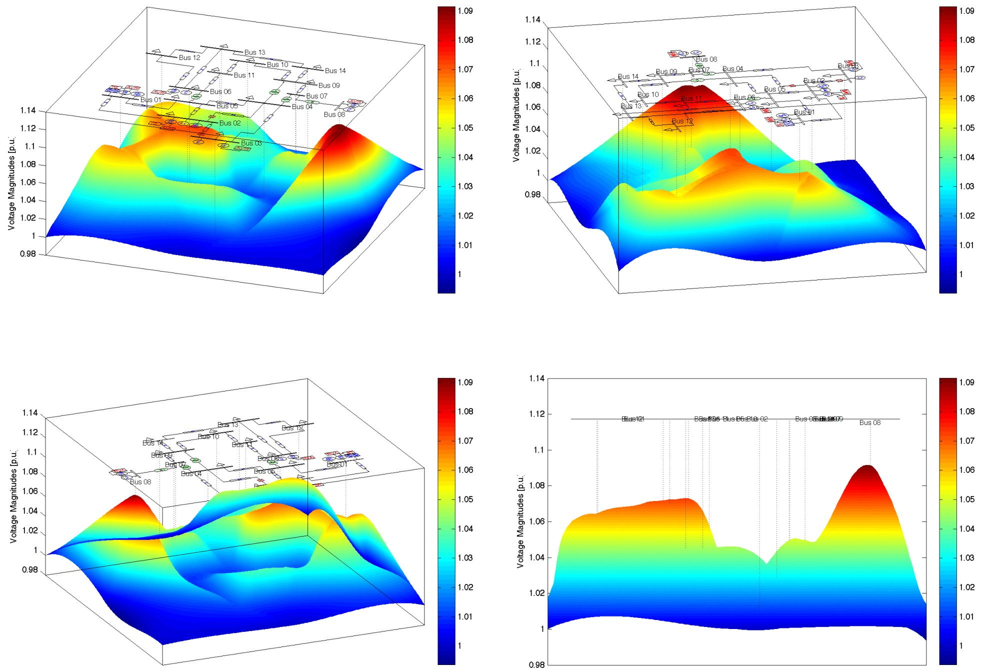

Fig. 2. A variety of points of view of the 3D voltage magnitude contour plot.

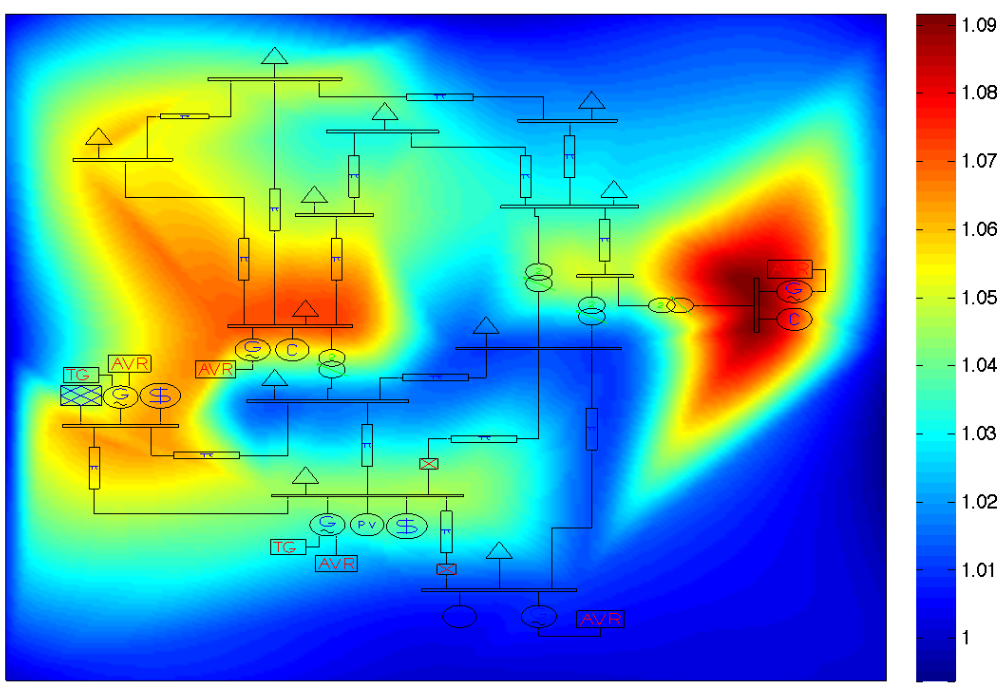

Fig. 3. 2D voltage magnitude contour plot.

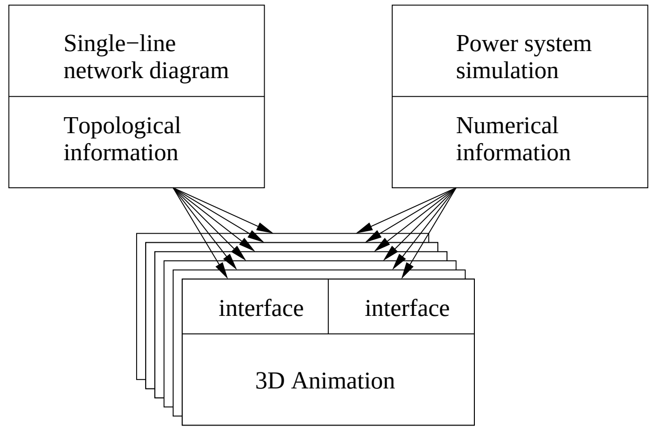

Fig. 4. Basic functioning of the 3D animation tool.

plots, but several frames are generated for each time step Δt in case of time domain simulations, or for each increment of the loading factor $\Delta\lambda$ in case of continuation power flow analyses. The frames are finally merged into a "movie" file. Some sample frames of such animations are presented in Section 3.

2.1 Features of the 3D Visualization and Animation

Human beings live in a 3D world that is constantly changing and moving. Thus, any attempt to visualize physical phenomena using a 3D environment is closer to every-day life than 2D static plots.

An important aspect that is difficult to "feel" from the reading of this paper is the fact that 3D maps are interactive, i.e. the user can rotate, zoom and manipulate the map. In a 3D map, "peaks" are generally easy to see, while "valleys" may be can remain hidden. However, rotating the 3D map allows viewing the map from all perspectives and creates in the user the impression of "flying" over the power system. Since one can see the map from any point of view, there is actually no part of the map that remains hidden.

Another aspect that cannot be properly shown in a paper is the effect of the animation of 3D maps during time domain integration or continuation power flow analysis. This is a pity, since the evolution of a 3D map is much clearer than simple color variations of a 2D contour map.

The visualization of large systems is also an important issue. More than the extension of the system, the issue is typically the level of the details. Very large systems with thousands of nodes appear messy in any representation, no matter if 2D or 3D. In the industry, this problem has been generally solved by creating a hierarchy of levels. At the top level, only HV nodes are visualized.

The operator can also visualize lower layers with the details of medium and low voltage buses. The same approach can be used for the 3D representation by zooming in and out the map. The interactive zooming process is very surprising although difficult to show in a paper. However, the purpose of the 3D approach is mainly for education. Thus large systems are generally not really an issue, since stability and control concepts can be better understood if dealing with systems with a reduced number of buses.

2.2 Didactic Experience and Student Feedback

The proposed 3D visualization and animation approach has been used for some undergraduate and graduate courses, as well as for seminars offered to practitioners.

The undergraduate course where the proposed 3D visualization has been experimented is a general-purpose power system course for civil engineers at the University of Castilla-La Mancha (academic course 2008-09). Since the students that attend this course are not expert in the field and only need a very basic preparation of electrical circuit, electric machines and power systems, the material is organized as brief seminars on relevant topics, such as design of low voltage feeders, transformers, synchronous machines, induction motor, etc. The goal is to provide to the students a qualitative overview of power systems. The seminar on synchronous machines explains the classical electromechanical model based on the pendulum analogy and shows the oscillations of the rotor angles and speeds of the generators of the WSCC 9-bus system using the 3D animations proposed in this paper.

The proposed 3D approach has proved to be very useful also for brief seminars about power system stability offered to practitioners and employees of transmission and system operators (e.g. a seminar offered by the author to the employees of Central America system operator in July 2008). The people that attend this kind of seminars are generally interested only in the qualitative aspects of stability. In this context, showing the representation of a voltage collapse or undamped oscillations through a 3D animation is more effective than explaining a standard bifurcation diagram or an eigenvalue loci.

3D simulations have been used also as complementary visual material to explain to the students of the Ph.D. course of the University of Castilla-La Mancha, Spain, and of a brief seminars on power system stability offered at Unicamp, Brazil, the concepts of inter-area oscillations, Hopf bifurcations and the effect of power system stabilizers.

Overall, the feedback from of students and practitioners is generally very positive. The 3D plots and animations stimulate the interest in the topic and motivate the student to go into the mathematical models and theory behind the simulations.

3 Examples and Comparison with Existing Plotting Tools

This section illustrates the proposed 3D visualization and animation approach through a variety of test networks. All simulations are solved using Matlab 7.5 on a Linux operating system. On a PC with 1 GB of RAM and 1.66 GHz Intel Core Duo Processor, generating the full 3D animations takes at most 1 minute, including simulation time. Thus, 3D animations are suitable for live demonstrations during classes or seminars. However, note that animations are for educational or training purposes and are not intended for on-line applications, thus computational time is actually not an issue. Simulations are based on an open source so that results can be freely reproduced by the interested reader [13]. Further details on this software tool are provided in Appendix A.

The following subsections depict results for the power flow analysis (Subsection 3.1), continuation power flow (Subsection 3.3), time domain simulation (Subsection 3.4), and optimal power flow (Subsection 3.2). Each analysis technique is briefly introduced at the beginning of each subsection and a comparison with traditional plots is provided.

3.1 Power Flow Analysis

The power flow problem is formulated as the solution of a nonlinear set of algebraic equations in the form:

$$\mathbf{0} = \boldsymbol{g}(\boldsymbol{y}, \boldsymbol{p}) \tag{1}$$

where $\boldsymbol{y}$ ($\boldsymbol{y} \in \mathbb{R}^m$) are the algebraic variables such as voltage amplitudes $\boldsymbol{v}$ and phases $\boldsymbol{\theta}$ at load buses, $\boldsymbol{p}$ ($\boldsymbol{p} \in \mathbb{R}^\ell$) are input parameters such as load powers, generator voltages and the slack bus reference angle, $\boldsymbol{g}$ ($\boldsymbol{g} : \mathbb{R}^m \times \mathbb{R}^\ell \rightarrow \mathbb{R}^m$) are the so-called power flow equations that ensure that active and reactive power balance at each network bus. The power flow problem is solved using the well-known Newton-Raphson algorithm, which is described in many books and papers (e.g. [14]).

Power flow results are typically given in forms of tables or bar plots (see Figure 5). From the observation of a table or of the bar plots, one cannot infer the topology of the system. The information is all there, but it is impossible to say at a glance which areas of the system are congested. To overcome this issue, in the control centers of power systems, practitioners typically use a topological

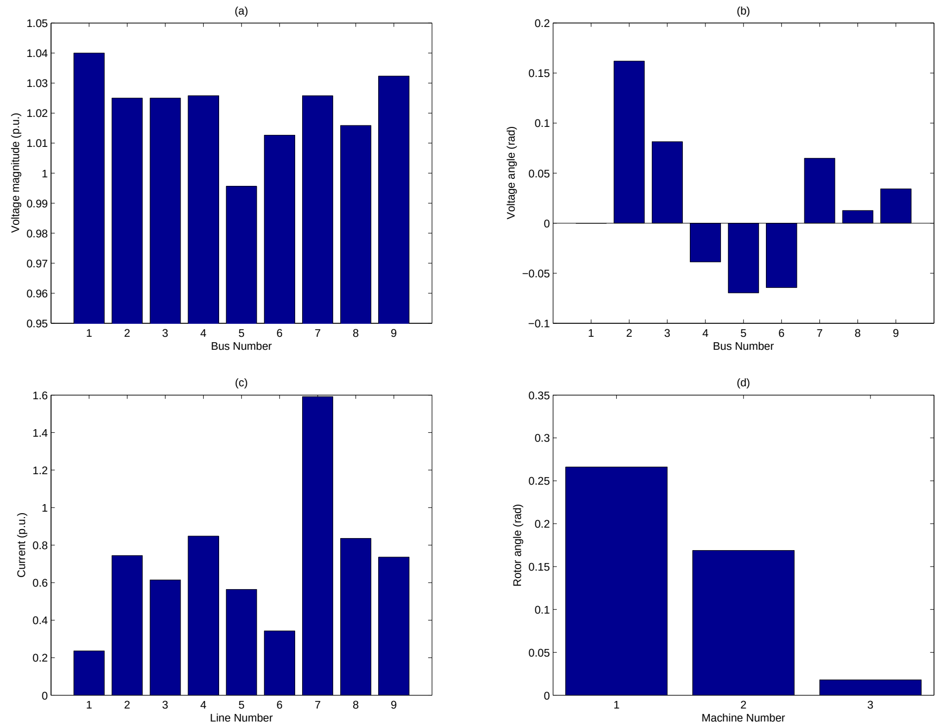

Fig. 5. Power flow analysis: standard bar plots for the WSCC 9-bus system: (a) bus voltage magnitudes; (b) bus voltage angles; (c) transmission line and transformer current flows; and (d) synchronous machines rotor angles.

scheme and the indication of bus voltage magnitudes and power flows. An example conceptually similar to what is typically used by system operators is shown in Figure 6. In this case, the topological information is preserved, but the user has still to read voltage values to understand whether some area is facing problems. In practice, low voltages are generally displayed in red or are blinking. Figure 7 depicts some 3D contour plots of the power flow analysis for the WSCC 9-bus system [15], namely bus voltage magnitudes; bus voltage angles; transmission line and transformer current flows; and synchronous machines rotor angles. Observe that 3D plots are able to provide both topological and technical information. Valleys are easily recognized as "depressed" regions (e.g., in the voltage plot) and hills possibly indicates congestion (e.g., in the line current flows).

3.2 Optimal Power Flow

The optimal power flow (OPF) is a static analysis, whose output is conceptually similar to the power flow, i.e., a single snapshot of power system functioning. In particular, the optimal power flow (OPF) problem is basically a nonlinear constrained optimization problem, and consists of a scalar objective function and a set of equality and inequality constraints. The OPF-based

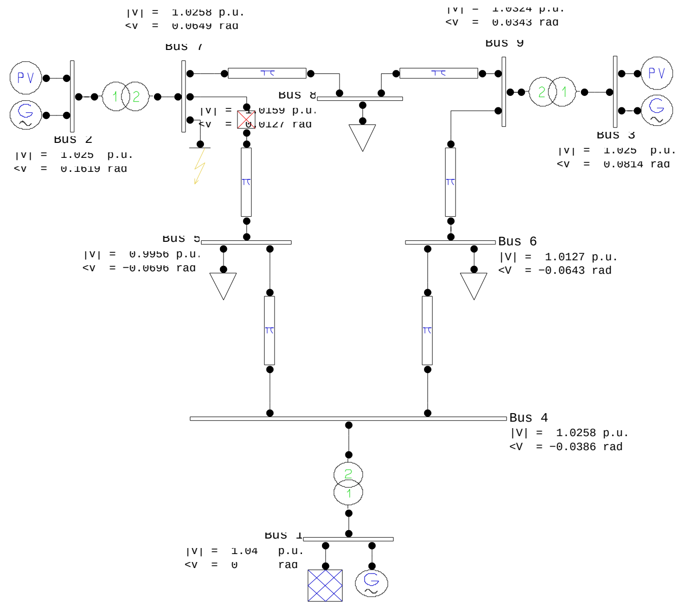

Fig. 6. Power flow analysis: topological scheme for the WSCC 9-bus system with indication of bus voltage magnitudes and phases.

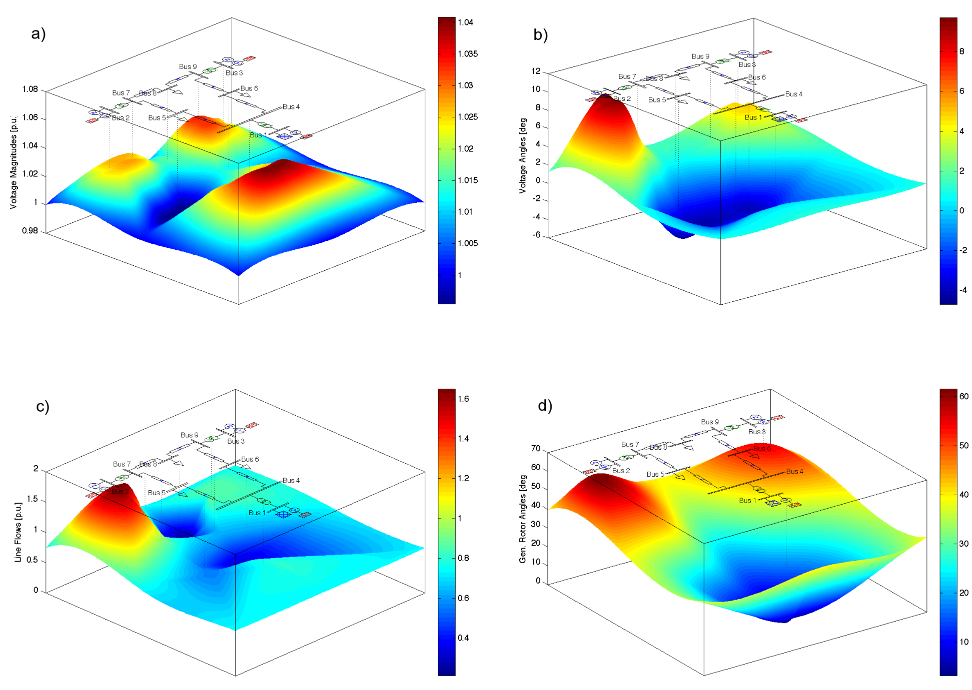

Fig. 7. Power flow analysis: 3D plots for the WSCC 9-bus system: (a) bus voltage magnitudes; (b) bus voltage angles; (c) transmission line and transformer current flows; and (d) synchronous machines rotor angles.

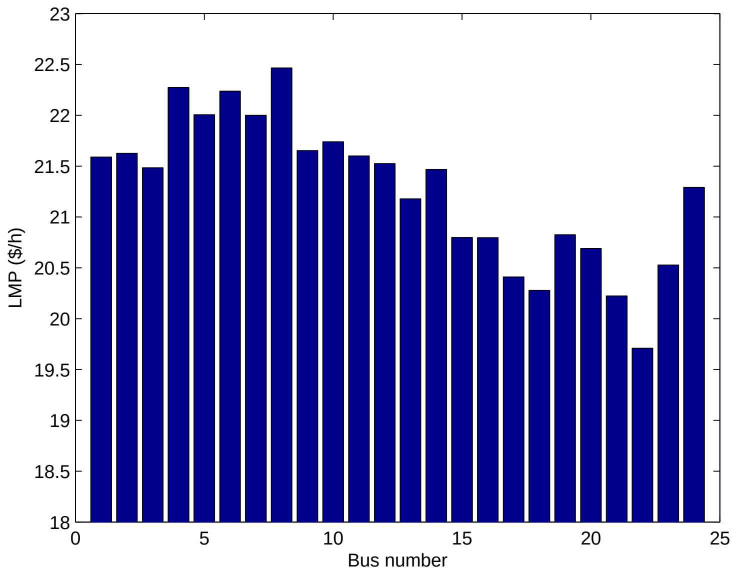

Fig. 8. Optimal power flow: standard bar plot of locational marginal prices for the RTS-96 system.

market model used in the following example is similar to that proposed in [16]:

$$
\begin{array}{rlcl}
\text{Min.} & -\left(\Sigma \boldsymbol{c}_D(\boldsymbol{p}_D) - \Sigma \boldsymbol{c}_S(\boldsymbol{p}_S)\right) & \rightarrow & \text{Social benefit} \\
\text{s.t.} & \boldsymbol{g}(\boldsymbol{\theta}, \boldsymbol{v}, \boldsymbol{q}_G, \boldsymbol{p}_S, \boldsymbol{p}_D) = \boldsymbol{0} & \rightarrow & \text{PF equations} \\
 & \boldsymbol{0} \leq \boldsymbol{p}_S \leq \boldsymbol{p}_S^{\max} & \rightarrow & \text{Sup. bid blocks} \\
 & \boldsymbol{0} \leq \boldsymbol{p}_D \leq \boldsymbol{p}_D^{\max} & \rightarrow & \text{Dem. bid blocks} \\
 & \boldsymbol{i}_{ij}(\boldsymbol{\theta}, \boldsymbol{v}) \leq \boldsymbol{i}_{ij}^{\max} & \rightarrow & \text{Thermal limits} \\
 & \boldsymbol{i}_{ji}(\boldsymbol{\theta}, \boldsymbol{v}) \leq \boldsymbol{i}_{ji}^{\max} & & \\
 & \boldsymbol{q}_G^{\min} \leq \boldsymbol{q}_G \leq \boldsymbol{q}_G^{\max} & \rightarrow & \text{Gen. } q \text{ limits} \\
 & \boldsymbol{v}^{\min} \leq \boldsymbol{v} \leq \boldsymbol{v}^{\max} & \rightarrow & v \text{ ``security'' limits}
\end{array}
\tag{2}
$$

where $\boldsymbol{c}_S$ and $\boldsymbol{c}_D$ are vectors of supply and demand bids in \$/MWh, respectively; $\boldsymbol{q}_G$ stand for the generator reactive powers; $\boldsymbol{v}$ and $\boldsymbol{\theta}$ are the bus phasor voltages; $\boldsymbol{i}_{ij}$ and $\boldsymbol{i}_{ji}$ are the currents flowing through the lines in both directions; and $\boldsymbol{p}_S$ and $\boldsymbol{p}_D$ are bounded supply and demand power bids in MW.

Since the OPF is a static analysis, results are traditionally shown as tables or bar charts, just as power flow results. For example, Figure 8 shows the locational marginal prices (LMPs) at each bus for the benchmark RTS-96 24-bus system [17]. Mathematically, LMPs are the dual variables associated to the active power flow equations. LMPs are relevant quantities for market participants, since LMPs indicate unambiguously how technical constraints affect economical transactions.

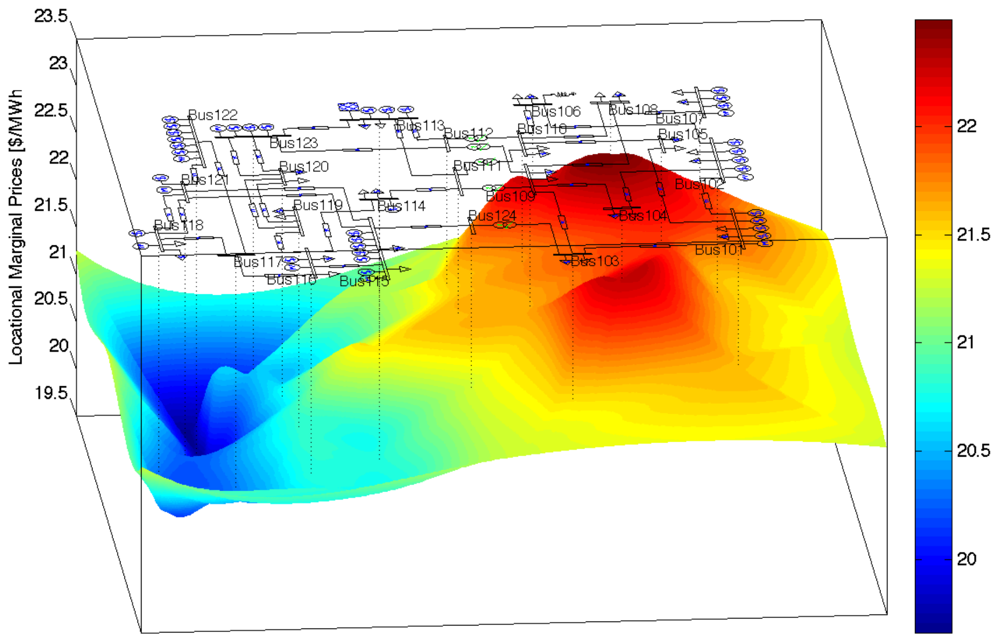

Fig. 9. Optimal power flow: 3D visualization of locational marginal prices for the RTS-96 system.

The OPF procedure, especially when dealing with electricity markets, is good example of "transverse" problem that merges together an engineering problem (power flow and security limits) with an economical one (e.g., maximization of the social benefit). Thus, it is not unlikely that engineers have to explain results to a non-engineer audience. In this case, the availability of an intuitive graphical interface can be of considerable help. Figure 9 depicts same LMPs as Fig 8, but using the proposed 3D visualization technique. The 3D plot is able to show at a very first glance which areas of the network are more expensive and which one are cheaper. This intuitive illustration cannot be obtained with a standard bar plot, where the network topology is completely neglected.

Of course, the plots of Figs. 7 and 9 could be displayed as 2D temperature maps, without loss of information. With respect to 2D maps, 3D surfaces have the advantage of been easily understood even by color-blind people. However, the main advantage of using 3D surfaces will be more evident in the next subsections that describe 3D animations for the continuation power flow analysis and time domain simulations.

The continuation power flow (CPF) analysis is used in voltage stability studies for computing Saddle-Node Bifurcation (SNB) points and Limit-Induced Bifurcation (LIB) points [18]. The CPF can be also used for determining voltage limits and flow limits of transmission lines.

CPF analysis requires steady-state equations of power system models, as follows:

$$\mathbf{0} = \boldsymbol{g}(\boldsymbol{y}, \boldsymbol{p}, \lambda) \tag{3}$$

where $\boldsymbol{y}$ are the algebraic variables (e.g., load bus voltage magnitudes and angles and generator bus voltage angles), $\boldsymbol{p}$ given parameters (e.g., $\boldsymbol{p}_G^0$ and $\boldsymbol{p}_S^0$ in (4) below) and λ, $\lambda \in \mathbb{R}$, is the *loading factor*, i.e. a scalar parameter that multiplies generator and load power directions, as follows:

$$\begin{aligned} \boldsymbol{p}_G &= \boldsymbol{p}_G^0 + (\lambda + k_G \boldsymbol{\gamma})\boldsymbol{p}_S^0 \\ \boldsymbol{p}_L &= \boldsymbol{p}_L^0 + \lambda \boldsymbol{p}_D^0 \\ \boldsymbol{q}_L &= \boldsymbol{q}_L^0 + \lambda \boldsymbol{q}_D^0 \end{aligned} \tag{4}$$

In (4), $\boldsymbol{p}_G^0$, $\boldsymbol{p}_L^0$ and $\boldsymbol{q}_L^0$ are the "base case" generator and load powers, whereas $\boldsymbol{p}_S^0$, $\boldsymbol{p}_D^0$ and $\boldsymbol{q}_D^0$ are the generator and load power directions. Finally, k_G is the distributed slack bus variable and $\boldsymbol{\gamma}$ are the generator participation coefficients. The CPF analysis consists in a predictor step realized by the computation of the tangent vector and in a corrector step that can be obtained either by means of a local parametrization or a perpendicular intersection [18, 19].

Conventional visualization of CPF results are the so-called "nose curves", i.e., plots of bus voltage magnitudes versus the loading factor λ. These curves exhibit a convex shape and allow determining the maximum value of the loading factor $\lambda^{\max}$, which is also known as the voltage collapse point. Figure 10 shows the bus voltage nose curves for the IEEE 14-bus system. While the information provided by the nose curves is quite clear, there are at least two main drawbacks in this standard visualization method. Firstly, only few curves can be displayed at a time, since too many curves can lead to a confused plot. The second issue is more subtle but maybe more important. When looking at a nose curve for the first time, one of the most common concern that students raise is why all bus voltages collapse at the same point. Actually, the loading factor λ is scalar and since the whole system is parametrized with respect to λ, all system variables necessarily collapse at $\lambda^{\max}$. However, this fact often generates perplexity in the students.

On the other hand, using a 3D animation, one can show, in a very intuitive way, how the whole system is affected by the loading factor variations. Figure

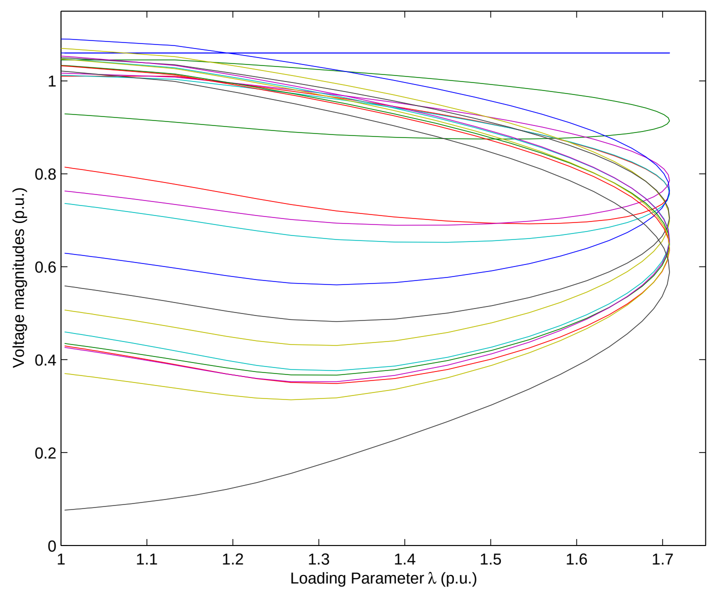

Fig. 10. Continuation power flow analysis: nose curves for the IEEE 14-bus system.

11 depicts four snapshots of the CPF analysis for the IEEE 14-bus system [20]. Figure 11.d shows the snapshot for $\lambda = 1.7073$, which is close to the collapse point. In this simulation, the voltage axes range is bounded to 1.1 and 0.9 p.u., respectively, so that the “quality” of the voltage profile is clear at a first glance: light blue, green, yellow and orange hues indicate a “sane” system, while dark red or dark blue colors indicate over or under voltages, respectively. Unfortunately, the snapshots do not fully illustrate the CPF analysis as the 3D animation does. The animation emphasizes the behavior of bus voltages, which slowly decrease as the loading factor increases up to very close to the critical bifurcation point, where most voltages suddenly collapse. In particular, the 3D animation clearly illustrates that the voltage collapse is a system-wide phenomena.

3.4 Time Domain Simulations

Time domain simulations are a conventional tool for power system analysis. The system is typically described through a set of differential-algebraic equations, as follows:

$$
\begin{aligned}
\dot{\boldsymbol{x}} &= \boldsymbol{f}(\boldsymbol{x}, \boldsymbol{y}, \boldsymbol{u}(t)) \\
\boldsymbol{0} &= \boldsymbol{g}(\boldsymbol{x}, \boldsymbol{y}, \boldsymbol{u}(t))
\end{aligned}
\tag{5}
$$

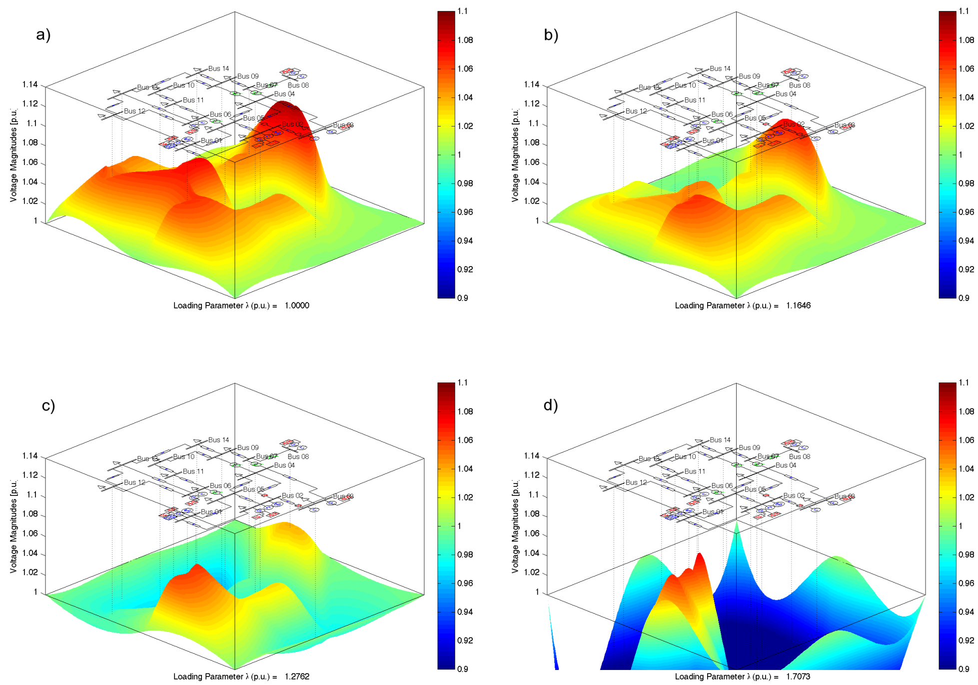

Fig. 11. Continuation power flow analysis: frames of the 3D animation for the IEEE 14-bus system: (a) $\lambda = 1.0000$; (b) $\lambda = 1.1646$; (c) $\lambda = 1.2762$; and (d) $\lambda = 1.7073$.

where most variable and equations have been defined in the previous subsections and $\boldsymbol{u}$ are input, possibly time dependent, variables. With the advances of computer speed, it is nowadays feasible to solve a time domain analysis even for real-size system with thousands of state variables. Stiff differential-algebraic equations such as power system ones can be efficiently solved by means of the trapezoidal rule, which is an implicit A-stable algorithm and uses a complete Jacobian matrix to evaluate the algebraic and state variable directions at each step. This method is well known and can be found in several books (e.g. [21]). As a matter of fact, the trapezoidal method is the workhorse solver for electromechanical DAE, and is widely used, in a variety of flavors, in most commercial and non-commercial power system software packages.

While the computational burden of numerical integration is not an issue with modern computers, an emerging issue is how to visualize the large amount of information that is provided by time domain simulations. Even for a small system, the amount of state and algebraic variables $\boldsymbol{x}$ and $\boldsymbol{y}$ that can be plotted versus the time is typically large. Especially for students, understanding the complete system behavior following a perturbation requires a certain grade of expertise.

Figure 12 shows a typical plot of synchronous machine rotor speeds for the WSCC 9-bus system [22]. This system has three synchronous machines de-

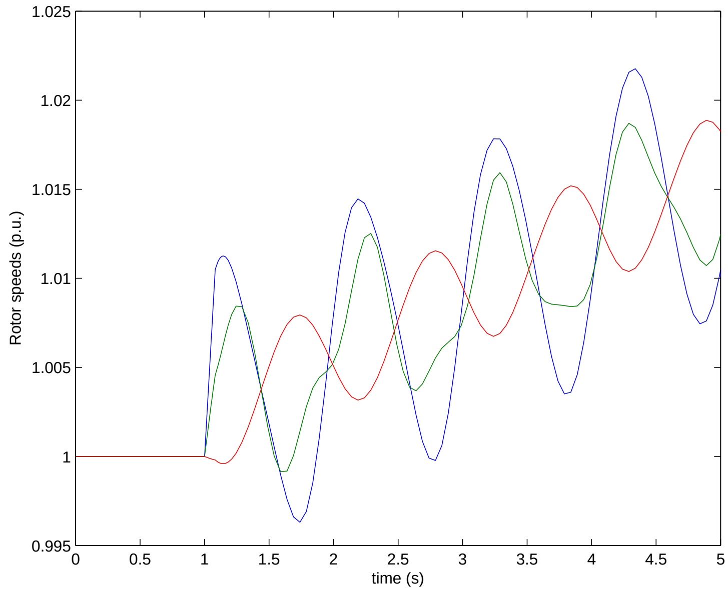

Fig. 12. Time domain simulation: conventional time domain plots of generator rotor speeds for the WSCC 9-bus system.

scribed by a simple second order model. The perturbation that causes rotor speed transients is a three phase fault that occurs at $t = 1$ s and is cleared after 83 ms. The most important concepts that the students should assimilate by Fig. 12 is (i) that rotor speed oscillations affect the whole system and (ii) that the oscillations of some machines is in counter-phase with respect of the rest of machines. The latter fact implies that following the fault clearance, the active power oscillates among synchronous machines. Conventional plots are able to show only that rotor speeds oscillate, but hardly show the picture of the whole system. This is mainly due to the lack of the topological information.

3D animations, more than variable time evolutions, can overcome this issue and help students to catch the system behavior. Figure 13 depicts four snapshots of the time domain simulation for the WSCC 9-bus example presented in [22]. The snapshots clearly show the post-fault oscillations of about 1 Hz of the rotor speeds. Once again, the 3D animation is much more illustrative than single snapshots. Observe that, once solved the simulation, the animation can be reproduced in real-time, thus allowing “feeling” system oscillations. In particular, the animation clearly shows how power “bounces” from one area to another of the system.

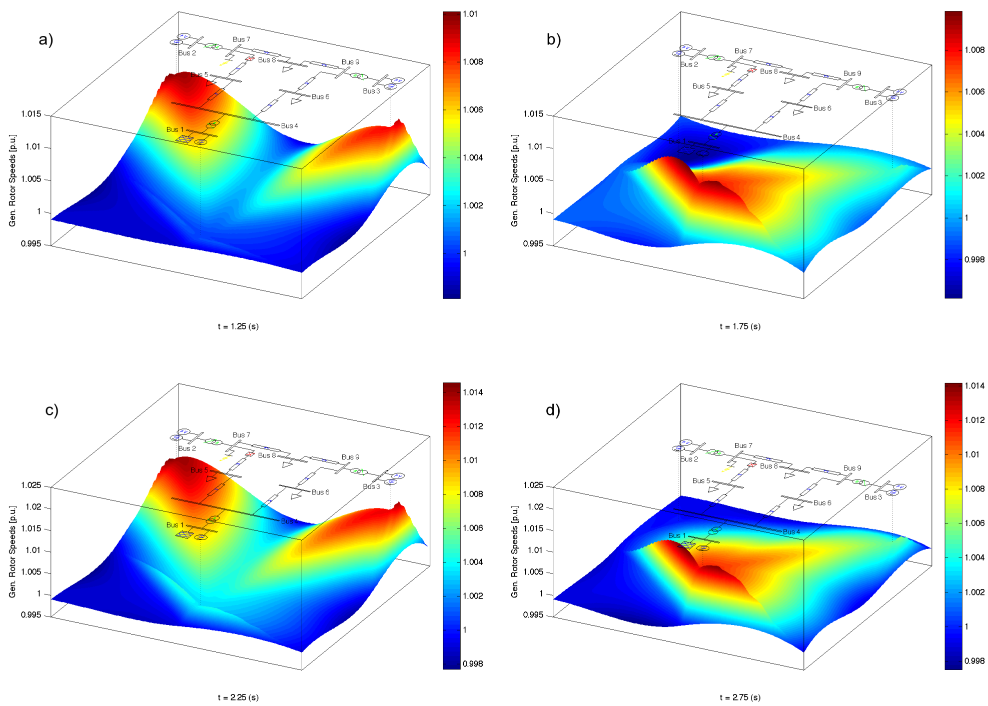

Fig. 13. Time domain simulation: frames of the 3D animation for the WSCC 9-bus system: (a) $t = 1.25$ s; (b) $t = 1.75$ s; (c) $t = 2.25$ s; and (d) $t = 2.75$ s.

4 Conclusions

The paper introduces 3D visualization and animation techniques for power systems analysis. Results of power flow analysis, continuation power flow, optimal power flow and time domain simulations are used for illustrating the proposed tool. The paper discusses with particular emphasis the applications of this technique for education and practitioner training. Future work will concentrate on the improvement of the 3D visualization and the development of new features for improving power system teaching. A promising development is the inclusion of GIS (geographic information system) technology in 3D maps.

A Outlines of the Software Tool

The simulations presented in this paper is based on PSAT, which is a Matlab-based software package for power system analysis [13]. In PSAT, the 3D visualization of power system simulations has been obtained using (i) the Simulink library that provides the topological description of the network [19]; and (ii) the 3D plot functions of the basic Matlab distribution [23]. Results of static

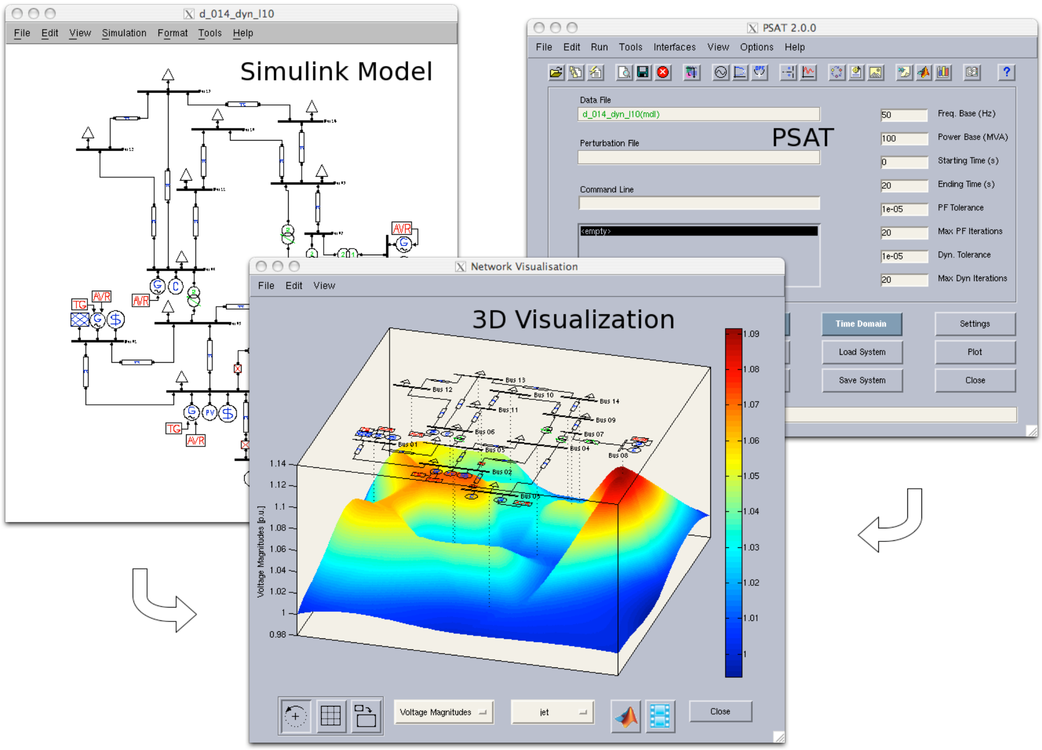

Fig. A.1. Implementation of the proposed tool for 3D visualization.

analyses, such as power flow or optimal power flow, are displayed as 3D contour plots, while time domain simulations and continuation power flow analysis produce 3D animations. The user can choose to display voltage magnitudes or angles, transmission line current flows, synchronous machine rotor speeds or angles, and locational marginal prices. Since PSAT is open source, it is possible to further extend and improve the 3D visualization. To the best of our knowledge, this is currently the only open source project that allows producing 3D maps and animations for power system analysis.

Figure A.1 gives a pictorial representation of the proposed tool. Observe that the Simulink library can be substituted with any other source of topological data, including Geographic Information Systems (GIS) [24]. One has just to create an interface to read the topological data into Matlab [23]. In a similar way, to solve power system analyses using PSAT is not strictly mandatory. As a matter of fact, PSAT provides interfaces to UWPFLOW [25] and GAMS [26]. Thus, given an adequate interface, the 3D module can be used to visualize results obtained from other power system software packages. Observe that modularity and extensibility is typical of the open source philosophy.

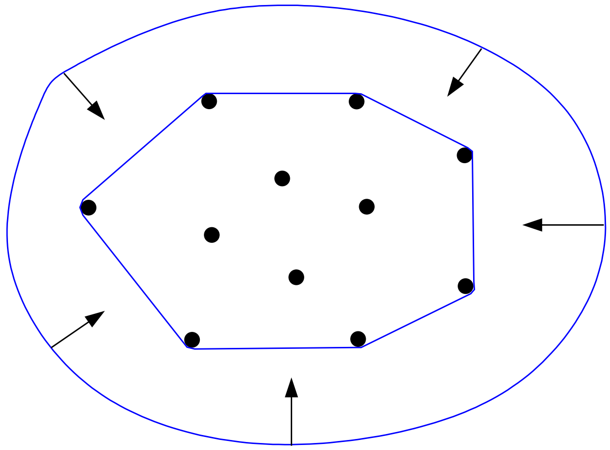

Fig. B.1. 2D representation of the convex hull [27].

B Outlines of the convex hull problem

This appendix provides brief outlines of the convex hull problem, which is used in this paper for determining the 3D surfaces that envelope the sets of electrical quantities. Most definitions and examples reported in this appendix are extracted from [27].

"The determination of the convex hull of a set of points is considered one of the most elementary interesting problem in computational geometry, just as minimum spanning tree is the most elementary interesting problem in graph algorithms" [27]. Roughly speaking, the convex hull captures the "shape" of a set of points or data. This is why the determination of the convex hull is so useful. Using mathematical terms, the convex hull for a set of points $\boldsymbol{X}$ in a real vector space $\boldsymbol{V}$ is the minimal convex set containing $\boldsymbol{X}$ [28].

The idea of convex hull can be easily visualized in two dimensions, i.e., for data sets that lie in the plane. In this case, the convex hull can be thought as an elastic band stretched open to encompass the given object. If released, the elastic band assumes the shape of the convex hull (see Fig. B.1).

The convex hull of a set $\boldsymbol{X}$ in a real vector space $\boldsymbol{V}$ certainly exists since $\boldsymbol{X}$ is contained at least in $\boldsymbol{V}$, which is a convex set. Furthermore, any intersection containing $\boldsymbol{X}$ is also a convex set containing $\boldsymbol{X}$. This fact, is useful for a mathematical definition of the convex hull. In particular, the Carathéodory's theorem states that the convex hull of $\boldsymbol{X}$ is the union of all simplexes with at most $n+1$ vertices from $\boldsymbol{X}$.

One can define the convex hull for any set composed of points in a vector space. The dimension of the data set can be any. However, the convex hull of finite sets of points in a two or three dimensions are the cases of most practical importance.

The determination of the convex hull is an important problem of computational geometry. Several algorithms with various computational burdens have been proposed for a finite set of points [29, 30]. The complexity of the corresponding algorithms is usually estimated in terms of n, the number of input points, and h, the number of points on the convex hull. In this paper, the 3D surfaces have been obtained using the `qhull` function, which is a general dimension code for computing convex hulls, Delaunay triangulations, and Voronoi diagrams [31].

The problem of finding convex hulls has several practical applications. Fields where the convex hull is widely used include, for example, pattern recognition, image processing, statistics and GIS. Furthermore, several important geometrical problems are based on the determination of the convex hull. For the sake of example, just think of the determination of the diameter given a set of points describing a circle is based on the convex hull. In fact, any diameter will always connect to points laying on the convex hull (e.g., the circumference) of the circle.

References

[1] P. M. Mahadev, R. D. Christie, Envisioning PowerSystem Data: Concepts and a Prototype System State Representation, IEEE Transactions on Power Systems 8 (3) (1993) 1084–1090.

[2] J. D. Weber, T. J. Overbye, Voltage Contours for Power System Visualization, IEEE Transactions on Power Systems 15 (1) (2000) 404–409.

[3] T. J. Overbye, D. A. Wiegmann, A. M. Rich, Y. Sun, Human Factors Aspects of Power System Voltage Contour Visualizations, IEEE Transactions on Power Systems 18 (1) (2003) 76–82.

[4] T. J. Overbye, J. D. Weber, K. J. Patten, Analysis and Visualization of Market Power in Electric Power Systems, in: Proceedings of the 32th Hawaii International Conference on System Sciences, Hawaii, 1999.

[5] T. J. Overbye, J. D. Weber, Visualizing Power System Data, in: Proceedings of the 33th Hawaii International Conference on System Sciences, Hawaii, 2000.

[6] T. J. Overbye, J. D. Weber, Visualizing the Electric Grid, IEEE Spectrum (2001) 52–58.

[7] R. P. Klump, J. D. Weber, Real-Time Data Retrieval and New Visualization Techniques for the Energy Industry, in: Proceedings of the 35th Hawaii International Conference on System Sciences, Hawaii, 2002.

[8] R. Klump, W. Wu, G. Dooley, Displaying Aggregate Data, Interrelated Quantities, and Data Trends in Electric Power Systems, in: Proceedings of the 36th Hawaii International Conference on System Sciences, Hawaii, 2003.

[9] Y. Sun, T. J. Overbye, Visualizations for Power System Contingency Analysis Data, IEEE Transactions on Power Systems 19 (4) (2004) 1859–1866.

[10] D. A. Wiegmann, T. J. Overbye, S. M. Hoppe, G. R. essemberg, Y. Sun, Human Factors Aspects of Three-Dimensional Visualization of Power System Information, in: Proceedings of the PES 2006 General Meeting, Montreal, 2006.

[11] N. Mithulananthan, C. A. C. nizares, J. Reeve, G. J. Rogers, Comparison of PSSS, SVC and STATCOM Controllers for Damping Power System Oscillations, IEEE Transactions on Power Systems 18 (2) (2003) 786–792.

[12] C. Y. Evrenosoğlu, A. Abur, E. Akleman, Three Dimensional Visualization and Animation of Travelling Waves in Power Systems, Electric Power System Research 77 (2007) 876–883.

[13] F. Milano, An Open Source Power System Analysis Toolbox, IEEE Transactions on Power Systems 20 (3) (2005) 1199–1206.

[14] W. F. Tinney, C. E. Hart, Power Flow Solution by Newton's Method, IEEE Transactions on Power Apparatus and Systems PAS-86 (1967) 1449–1460.

[15] P. W. Sauer, M. A. Pai, Power System Dynamics and Stability, Prentice Hall, Upper Saddle River, New Jersey, 1998.

[16] K. Xie, Y.-H. Song, J. Stonham, E. Yu, G. Liu, Decomposition Model and Interior Point Methods for Optimal Spot Pricing of Electricity in Deregulation Environments, IEEE Transactions on Power Systems 15 (1) (2000) 39–50.

[17] Reliability Test System Task Force of the Application of Probability Methods subcommittee, The IEEE Reliability Test System - 1996, IEEE Transactions on Power Systems 14 (3) (1999) 1010–1020.

[18] C. A. Cañizares, Voltage Stability Assessment: Concepts, Practices and Tools, Tech. rep., IEEE/PES Power System Stability Subcommittee, Final Document, available at http://www.power.uwaterloo.ca (Aug. 2002).

[19] F. Milano, PSAT, Matlab-based Power System Analysis Toolbox, available at http://www.uclm.es/area/gsee/Web/Federico (2007).

[20] IEEE Power Systems Test Case Archive, available at http://www.ee.washington.edu/research/pstca/.

[21] K. E. Brenan, S. L. Campbell, L. Petzold, Numerical Solution of Initial-Value Problems in Differential-Algebraic Equations, SIAM, Philadelphia, PA, 1995.

[22] P. M. Anderson, A. A. Fouad, Power System Control and Stability, The Iowa State University Press, Ames, Iowa, 1977.

[23] The MathWorks, Inc., Matlab Programming, available at http://www.mathworks.com (2005).

[24] Geographic Information Systems, available at http://www.gis.com.

[25] C. A. Cañizares, F. L. Alvarado, UWPFLOW Program, university of Waterloo, available at http://www.power.uwaterloo.ca (2000).

[26] A. Brooke, D. Kendrick, A. Meeraus, R. Raman, R. E. Rosenthal, GAMS, a User's Guide, GAMS Development Corporation, 1217 Potomac Street, NW, Washington, DC 20007, USA, available at http://www.gams.com/ (Dec. 1998).

[27] S. S. Skiena, The Algorithm Design Manual, Springer-Verlag, New York, 1998.

[28] F. P. Preparata, S. J. Hong, Convex Hulls of Finite Sets of Points in Two and Three Dimensions, Commun. ACM 20 (2) (1977) 87–93.

[29] T. H. Cormen, C. E. Leiserson, R. L. Rivest, C. Stein, Introduction to Algorithms, MIT Press and McGraw-Hill, 2001.

[30] M. de Berg, M. van Kreveld, M. Overmars, O. Schwarzkopf, Computational Geometry, Algorithms and Applications, Springer, 2000.

[31] Qhull, available at http://www.qhull.org.